

Charged multiplicity distributions in deep inelastic scattering at HERA

ZEUS Collaboration

Abstract

The hadronic final state has been investigated in inclusive neutral current deep inelastic ep scattering with the ZEUS detector at HERA, using an integrated luminosity of 38.6 pb^{-1} . The mean charged multiplicity observed in the pseudorapidity region $|\eta_{\text{lab}}| \leq 1.75$ has been measured as a function of its invariant mass, M_{eff} . This dependence has been also measured for the hadrons belonging to the current and target regions of the Breit frame. For the current region of the Breit frame the mean charged multiplicity multiplied by two is measured versus twice the total energy of the respective particles. The results are compared to leading-logarithm parton-shower Monte Carlo predictions as well as to e^+e^- measurements.

1 Introduction

The measurements of multiplicities of charged particles at colliders have yielded insights into hadronization mechanisms. It has been found that charged particle multiplicities measured as a function of the centre-of-mass (cms) energy, \sqrt{s} , at e^+e^- [1] colliders are the same as those measured at pp [2] colliders as a function of $\sqrt{q_{\text{tot}}^{\text{had}}} = \sqrt{[(q_1^{\text{inc}} - q_1^{\text{leading}}) + (q_2^{\text{inc}} - q_2^{\text{leading}})]^2}$, where $q_{1,2}^{\text{inc}}$ and $q_{1,2}^{\text{leading}}$ are the four-momenta of the incoming protons and leading particles that escape down the beampipe, respectively. It is therefore interesting to study charged particle multiplicities in ep collisions.

The measurement of the total number of particles produced in an ep collision as a function of the γP cms energy, W , is experimentally difficult. The beam configuration is highly asymmetric and a large part of the hadronic system falls outside the region of acceptance of the detectors.

To perform studies similar to e^+e^- and pp also in ep collisions at HERA, only the visible part of the hadronic system is used in this analysis. The mean charged multiplicity is studied as a function of the respective invariant mass, M_{eff} . The study is performed in the laboratory frame and in the current and target regions of the Breit frame.

2 Experimental set-up

The data were collected with the ZEUS detector during the 1996 and 1997 running periods, when HERA operated with protons of energy $E_p = 820$ GeV and positrons of energy $E_e = 27.5$ GeV, and correspond to an integrated luminosity of 38.6 ± 0.6 pb $^{-1}$.

The ZEUS detector is described in detail elsewhere [3]. The most important components used in the current analysis are the central tracking detector (CTD), and the uranium-scintillator calorimeter (CAL).

Charged particles are tracked in the central tracking detector (CTD) [4], which operates in a magnetic field of 1.43 T provided by a thin superconducting coil. The CTD consists of 72 cylindrical drift chamber layers, organized in 9 superlayers covering the polar-angle¹ region $15^\circ < \theta < 164^\circ$. The transverse-momentum resolution for full-length tracks is $\sigma(p_T)/p_T = 0.0058p_T \oplus 0.0065 \oplus 0.0014/p_T$, with p_T in GeV.

The high-resolution uranium-scintillator calorimeter (CAL) [5] consists of three parts: the forward (FCAL), the barrel (BCAL) and the rear (RCAL) calorimeters. Each part

¹ The ZEUS coordinate system is a right-handed Cartesian system, with the Z axis pointing in the proton beam direction, referred to as the “forward direction”, and the X axis pointing left towards the centre of HERA. The coordinate origin is at the nominal interaction point.

is subdivided transversely into towers and longitudinally into one electromagnetic section (EMC) and either one (in RCAL) or two (in BCAL and FCAL) hadronic sections (HAC). The smallest subdivision of the calorimeter is called a cell. The CAL energy resolutions, as measured under test-beam conditions, are $\sigma(E)/E = 0.18/\sqrt{E}$ for electrons and $\sigma(E)/E = 0.35/\sqrt{E}$ for hadrons (E in GeV).

3 Data selection

Deep inelastic scattering (DIS) events were selected by requiring that the outgoing positron was measured in the CAL. The scattered-positron identification is based on a neural-network algorithm using the CAL information [6].

For the reconstruction of the photon virtuality, Q^2 , Bjorken x , and the γ^*P centre-of-mass energy, W , the double angle method (DA) was chosen, in which the scattered-positron angle, θ_e , and the angle γ_H are used [7]. In the naive quark-parton model, γ_H is the angle of the scattered massless quark in the laboratory frame. Variables calculated by electron method (e) [7] from the measurements of the energy, $E_{e'}$, and angle, $\theta_{e'}$, of the scattered positron and by the Jacquet-Blondel (JB) method [8] from the hadronic system measurements were used only in the event selection.

The event selection criteria were:

- $E_{e'} > 12$ GeV, where ($E_{e'}$ is the corrected energy of the scattered positron), to select neutral current DIS events;
- $y_e \leq 0.95$, where y_e is the scaling variable y as determined from the energy and polar angle of the scattered positron, to reduce the photoproduction background;
- $y_{\text{JB}} \geq 0.04$, where $y_{\text{JB}} = \sum_h (E_h - P_{Z_h})/2E_e$ and the sum runs over all the observed hadrons, E_h and P_{Z_h} are the energies and longitudinal momenta of these hadrons correspondingly, to guarantee sufficient accuracy for the DA reconstruction method;
- $35 \leq \delta \leq 60$ GeV, where $\delta = \sum_i (E_i - P_{Z_i})$ and the sum runs over the energies and longitudinal momenta of all calorimeter cells. This cut removes photoproduction events and events with large radiative corrections;
- events were accepted only if the impact position of the scattered positron on the CAL satisfied $\sqrt{X^2 + Y^2} > 25$ cm to ensure that the positron is fully contained within the detector and its position reconstructed with sufficient accuracy;
- $|Z_{\text{vertex}}| < 50$ cm to reduce background events from non ep -collisions;
- events with $\eta^{\text{max}} > 3.2$ were rejected to reduce diffractive contributions, where η^{max} is the pseudorapidity of the most forward energy deposit in the CAL.

The track selection was as follows:

- the reconstructed tracks were associated with the primary event vertex;
- the tracks were required to have $p_T > 150$ MeV to reduce errors due to misreconstruction;
- $|\eta_{\text{lab}}| < 1.75$, where η is the pseudorapidity of the measured track. This cut restricts the analysis to a region of high CTD acceptance where the detector response and systematics are best understood. It also excludes the region of the proton remnant.

The selection cuts restrict the analysis to the range $25 < Q^2 < 1200$ GeV² and $70 < W < 225$ GeV. After all event selection 735007 DIS events remained for further analysis.

4 Analysis method

For this analysis, the CTD was used to measure the charged-particle multiplicity and the CAL to measure the energy and momenta of the final-state hadrons (charged and neutral) in the same geometrical region as used for the CTD. Calorimeter cells and the track assigned to the scattered positron were not used in these measurements.

The invariant mass of the final state hadronic system, M_{eff} , was reconstructed from the energy and momenta of the hadrons as:

$$M_{\text{eff}}^2 = \left(\sum_i E_i\right)^2 - \left(\sum_i P_{X_i}\right)^2 - \left(\sum_i P_{Y_i}\right)^2 - \left(\sum_i P_{Z_i}\right)^2, \quad (1)$$

where the sum runs over the calorimeter energy flow objects [9] (EFOs) or hadrons of the system, in the case of hadron level MC.

Measurements were performed in the laboratory and in the Breit [10] frames. In the Breit frame, the exchanged virtual boson is purely spacelike, with three-momentum $\mathbf{q} = (0,0,-Q)$. The particles produced in the interaction can be assigned to one of two regions: the current region if their z -momentum in the Breit frame is negative, and the target region if their z -momentum is positive. The main advantage of this frame is that it gives maximal separation of the incoming and outgoing partons in the quark-parton model (QPM). Another advantage of the Breit frame is that the hadronic system of the current region used in this analysis is almost fully contained within the acceptance of the CTD.

The boost to the Breit frame was performed using the positron four-momentum as reconstructed using the DA method. The total energy for the current frame particles, E_{current} , was calculated as the sum of the energies of the boosted particles in the current region.

5 Monte Carlo models, acceptance corrections and systematic errors

Samples of neutral current DIS events were generated using the HERACLES 4.6.1 [11] MC program with the DJANGO 1.1 [7] interface to the hadronisation programs. The QCD cascade is simulated using the colour-dipole model as implemented in ARIADNE 4.08 [12] or with the MEPS model of LEPTO 6.5 [13]. Both ARIADNE and LEPTO use the Lund string model [14] for the hadronisation. Two samples of LEPTO were generated, one of which included contributions from soft-colour-interactions (SCI). All event samples were generated using the CTEQ4D parameterisation of the parton distribution functions in the proton.

The MC event samples were passed through reconstruction and selection procedures identical to those for the data. Monte Carlo studies were used to determine the event and track acceptances as a function of M_{eff} in the selected kinematic region of Q^2 and W^2 .

The corrections applied to the data accounted for the effects of acceptance and resolution of the detector, event selection cuts, QED-radiative effects, track reconstruction, track selection cuts, the decay products of K_S^0 and Λ which were assigned to the primary vertex, and energy losses in the inactive material in front of the calorimeter in the case of the M_{eff} determination.

The average values of M_{eff} and E_{current} in each bin were corrected using a bin-by-bin correction technique. Two correction procedures for the multiplicity distributions were used. One of them is based on the matrix unfolding method as used in earlier studies [15]. The second is a bin-by-bin method. Both methods give similar results. The difference between them is included as a systematic uncertainty.

The generated hadron distributions do not include charged particles produced from weak decays with lifetimes below $3 \cdot 10^{-10}$ seconds. For the measurements where the data are compared to e^+e^- measurements (Fig. 1), the charged-particle decay products of K_S^0 and Λ were also excluded. The exclusion of decay particles from K_S^0 and Λ causes a difference of a few percent in the total number of charged hadrons.

The dominant sources of systematic uncertainties were investigated. They arise from (typical values of the uncertainties are shown in brackets): uncertainty in the CAL energy scale (0.5 – 1.1%), event reconstruction and selection (< 0.5%), track reconstruction and selection (< 0.5%), MC model used in the correction procedure (< 0.5%), and method of correction (matrix or modified bin-by-bin, 0.6 – 1.3%). The contributions from photo-production and diffractive events are negligible.

6 Results

All data presented in this section have been corrected for detector and acceptance effects according to the procedure described in Section 5.

6.1 Breit frame analysis and comparison to e^+e^-

The current region of the Breit frame is analogous to a single hemisphere of e^+e^- annihilation. In $e^+e^- \rightarrow q\bar{q}$ the two quarks are produced with equal and opposite momenta, $\pm\sqrt{s_{ee}}/2$. The fragmentation of these quarks can be compared to that of the quark struck from the proton. This quark has an outgoing momentum $-Q/2$ in the Breit frame. Two times the multiplicity of the current region of the Breit frame is expected to have a dependence on Q similar to that of the total multiplicity in e^+e^- annihilation versus the energy $\sqrt{s_{ee}} = Q$. To take into account contributions from soft and hard QCD processes that lead to decrease of the energy and the number of particles in the current region of the Breit frame, in this analysis E_{current} was used instead of $Q/2$, where E_{current} is the energy of all the particles in the current region of the Breit frame.

Figure 1 shows twice the measured mean charged multiplicity, $2\langle n_{\text{ch}} \rangle$, in the current region of the Breit frame plotted versus $2E_{\text{current}}$. Also shown are the prediction of ARIADNE and the measurements from e^+e^- and hadron-hadron experiments together with a previous ZEUS measurement in the current region of the Breit frame. For the previous ZEUS measurement [16], $2 \cdot \langle n_{\text{ch}} \rangle$ is measured as a function of Q . Both ZEUS measurements agree with the e^+e^- measurement for values of energy above 10 GeV. At low values of energy, the measurement as a function of $2E_{\text{current}}$ agrees better with e^+e^- than the measurement as a function of Q . The migrations of final state particles out of the current region are larger at the low values of energy and they are properly taken into account in E_{current} .

Similarly to \sqrt{s} , $2E_{\text{current}}$ constitutes not only the energy but also the invariant mass of the system. It is natural to use the invariant mass as a scale for comparison of the mean charged multiplicities in the current and target region of the Breit frame. But while almost 95% of the hadronic system of the current region is measured in the ZEUS detector, only $\sim 25\%$ is detected in the case of the target region. The measurement here are performed for the visible charged multiplicity as a function of the visible invariant mass M_{eff} in the way explained in section 4.

For the target region, the invisible part of the system belongs mainly to the region close to the proton remnant. MC studies with ARIADNE showed a significant decrease in the number of charged particles as a function of M_{eff} if the pseudorapidity range was increased

to include regions close to the proton. Such an effect cannot unfortunately be confirmed experimentally because of the acceptance restrictions of the detector.

Figure 2 shows the measured $\langle n_{\text{ch}} \rangle$ for the visible part of the current and target regions of the Breit frame versus the respective M_{eff} . The measurement shows approximately the same number of particles produced for the same M_{eff} in the visible part of the current and target regions. Because of the energy restrictions, the highest achievable M_{eff} in the current region is smaller than that for the target region. The laboratory frame measurement (combined current+target) is also shown as well as the predictions for each region of the Breit frame. ARIADNE describes the measurements for both the current and target regions of the Breit frame.

Since both the number of particles and M_{eff} are Lorentz boost invariant, the study of the total visible multiplicities is continued in the laboratory frame.

6.2 Multiplicity distributions in the laboratory frame

Figure 3 shows the measured charge multiplicity, $\langle n_{\text{ch}} \rangle$, for the visible part of the laboratory frame as a function of the respective M_{eff} . The predictions from ARIADNE, LEPTO, and LEPTO including SCI are also shown. ARIADNE describes the data better, while LEPTO and LEPTO with the SCI are above the data. Similar behaviour of ARIADNE and LEPTO has been observed in previous measurements [16].

Figure 4 shows $\langle n_{\text{ch}} \rangle$ as a function of M_{eff} in the laboratory frame for different x regions together with predictions from ARIADNE. A weak x dependence is observed both in data and MC.

Figure 5 shows $\langle n_{\text{ch}} \rangle$ as a function of M_{eff} in the laboratory frame for different Q^2 and x regions together with ARIADNE and LEPTO predictions for those (x, Q^2) regions. Also the prediction of ARIADNE for the total phase space (the ARIADNE prediction of Fig. 3) is shown in each (x, Q^2) region. No Q^2 dependence is observed.

7 Summary and conclusions

The hadronic final state has been investigated in inclusive neutral current deep inelastic ep scattering in terms of the mean charged multiplicity and the respective invariant mass of the charged and neutral particles M_{eff} .

Measurements in the current region of the Breit frame showed the same dependence as in the case of e^+e^- measurements if $2E_{\text{current}}$ was used as the scale.

Similar dependence was observed in the charged current multiplicities for the visible parts of current and target regions of the Breit frame as a function of their respective effective masses.

The measurement in the laboratory frame showed no strong dependence versus x and Q^2 .

References

- [1] MARK I Coll., V. Luth et al., Phys. Lett. **B 70**, 120 (1977);
JADE Coll., W. Bartel et al., Z. Phys. **C 20**, 187 (1983).
- [2] M. Basile et al., Nuovo Cimento **A 67**, 244 (1982);
M. Basile et al., Lettere al Nuovo Cimento 41 **N. 9**, 293 (1984).
- [3] ZEUS Coll., U. Holm (ed.), *The ZEUS Detector*. Status Report (unpublished),
DESY (1993), available on <http://www-zeus.desy.de/bluebook/bluebook.html>.
- [4] N. Harnew et al., Nucl. Inst. Meth. **A 279**, 290 (1989);
B. Foster et al., Nucl. Phys. Proc. Suppl. **B 32**, 181 (1993);
B. Foster et al., Nucl. Inst. Meth. **A 338**, 254 (1994).
- [5] M. Derrick et al., Nucl. Inst. Meth. **A 309**, 77 (1991);
A. Andresen et al., Nucl. Inst. Meth. **A 309**, 101 (1991);
A. Caldwell et al., Nucl. Inst. Meth. **A 321**, 356 (1992);
A. Bernstein et al., Nucl. Inst. Meth. **A 336**, 23 (1993).
- [6] H. Abramowicz, A. Caldwell and R. Sinkus, Nucl. Inst. Meth. **A 365**, 508 (1995).
- [7] S. Bentvelsen, J. Engelen and P. Kooijman, *Proc. Workshop on Physics at HERA*,
W. Buchmüller and G. Ingelman (eds.), Vol. 1, p. 23. Hamburg, Germany, DESY
(1992);
K.C. Höger, *Proc. Workshop on Physics at HERA*, W. Buchmüller and
G. Ingelman (eds.), Vol. 1, p. 43. Hamburg, Germany, DESY (1992).
- [8] F. Jacquet and A. Blondel, *Proc. the Study of an eP Facility for Europe*,
U. Amaldi (ed.), p. 391. (1979). Also in preprint DESY 79-48.
- [9] G.M. Briskin, *Diffractional Dissociation in ep Deep Inelastic Scattering*. Ph.D.
Thesis, Tel Aviv University, 1998. (Unpublished).
- [10] R.P. Feynman, *Photon-Hadron Interactions*. Benjamin, New York, 1972.
- [11] A. Kwiatkowski, H. Spiesberger and H.-J. Möhring, Comp. Phys. Comm.
69, 155 (1992). Also in *Proc. Workshop Physics at HERA*, 1991, DESY, Hamburg;
H. Spiesberger, *An Event Generator for ep Interactions at HERA Including
Radiative Processes (Version 4.6)*, 1996, available on
<http://www.desy.de/~hspiesb/heracles.html>;
H. Spiesberger, *HERACLES and DJANGO: Event Generation for ep Interactions at
HERA Including Radiative Processes*, 1998, available on
<http://www.desy.de/~hspiesb/djangoh.html>;
K. Charchula, G.A. Schuler and H. Spiesberger, Comp. Phys. Comm.
81, 381 (1994).

- [12] L. Lönnblad, *Comp. Phys. Comm.* **71**, 15 (1992).
- [13] G. Ingelman, A. Edin and J. Rathsman, *Comp. Phys. Comm.* **101**, 108 (1997).
- [14] B. Andersson et al., *Phys. Rep.* **97**, 31 (1983).
- [15] ZEUS Coll., M. Derrick et al., *Z. Phys.* **C 67**, 93 (1995).
- [16] ZEUS Coll., J. Breitweg et al., *Eur. Phys. J.* **C 11**, 251 (1999).

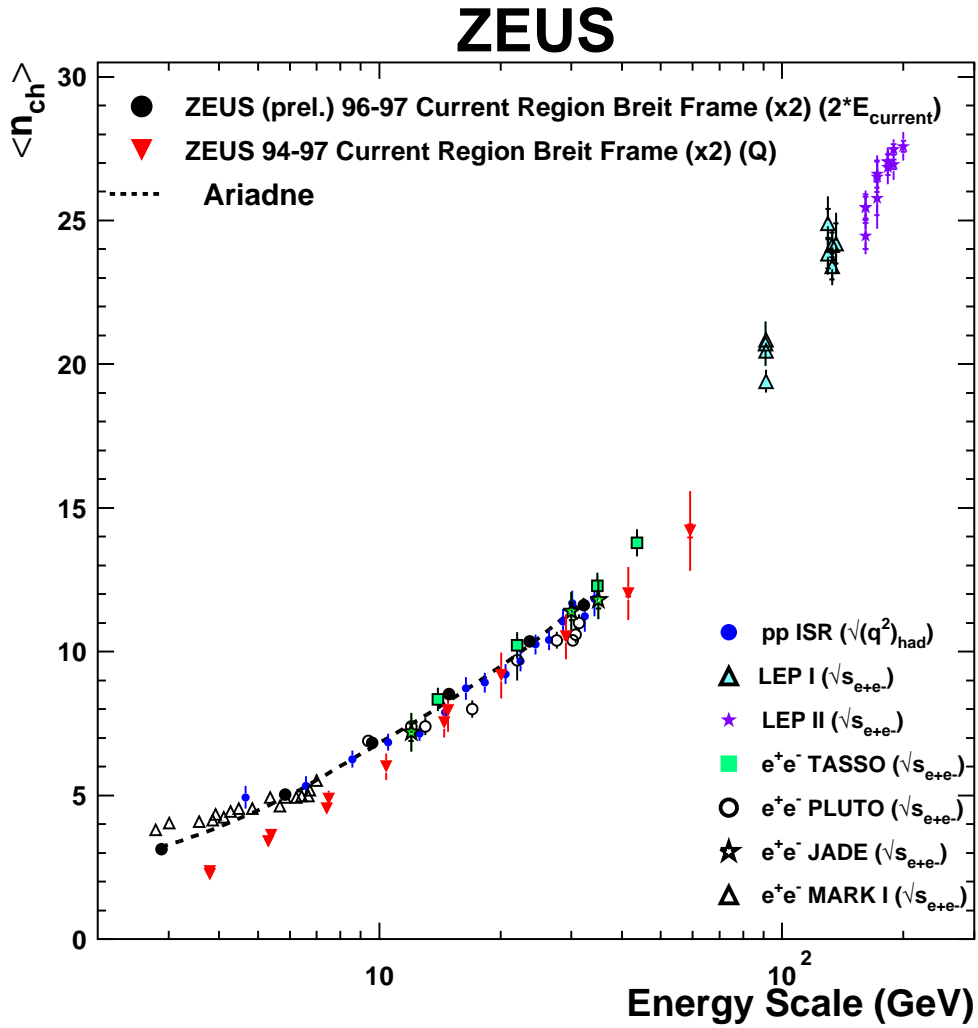


Figure 1: Mean charged multiplicity, $\langle n_{\text{ch}} \rangle$, in the current region of the Breit frame multiplied by 2 plotted versus $2E_{\text{current}}$, where E_{current} is the sum of the energies of the particles in the current region (charged hadrons and neutrals). Also shown are the prediction from ARIADNE and other measurements from hadron-hadron, e^+e^- , and ep.

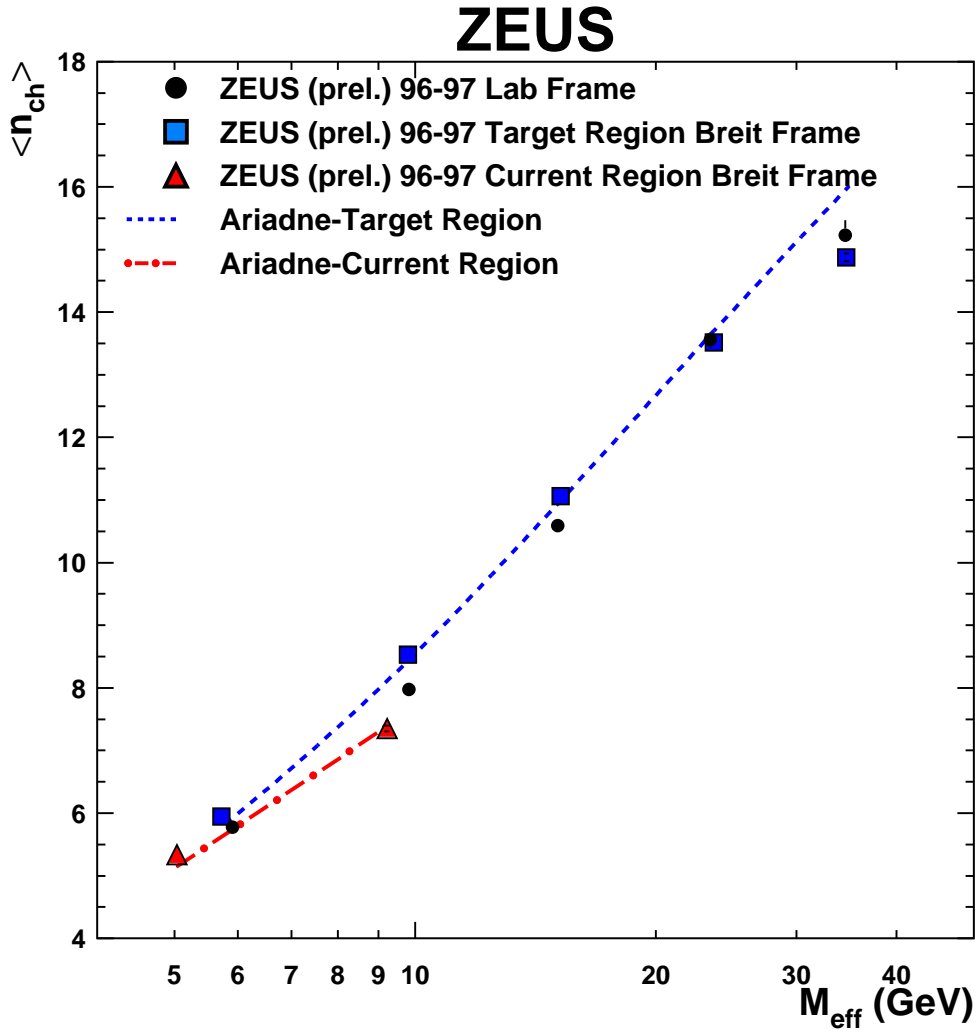


Figure 2: $\langle n_{ch} \rangle$ in the current and target regions of the Breit frame versus the M_{eff} of the respective (charged + neutral) particles together with the laboratory frame measurement (combined current+target). The predictions from ARIADNE for both regions of the Breit frame are also shown.

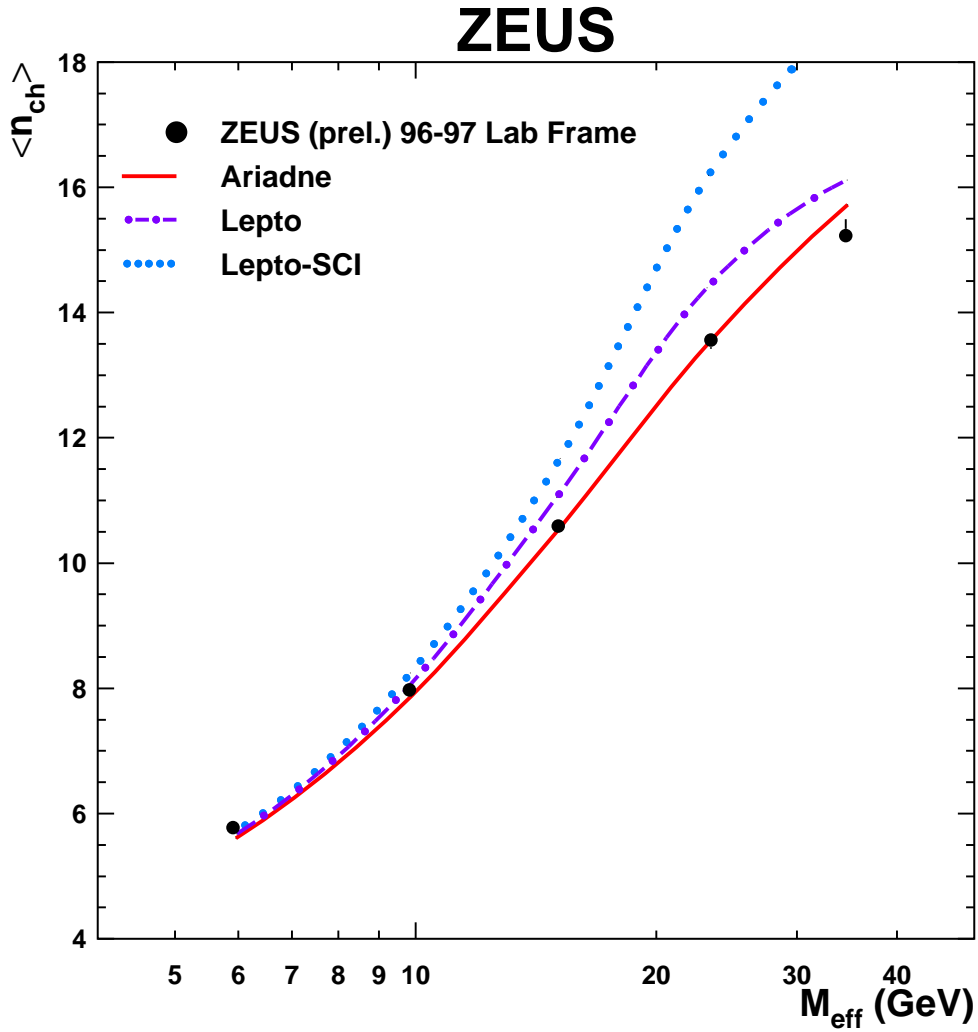


Figure 3: $\langle n_{\text{ch}} \rangle$ in the laboratory frame versus the M_{eff} of the respective (charged + neutral) particles. The predictions from ARIADNE, LEPTO, and LEPTO including SCI are also shown.

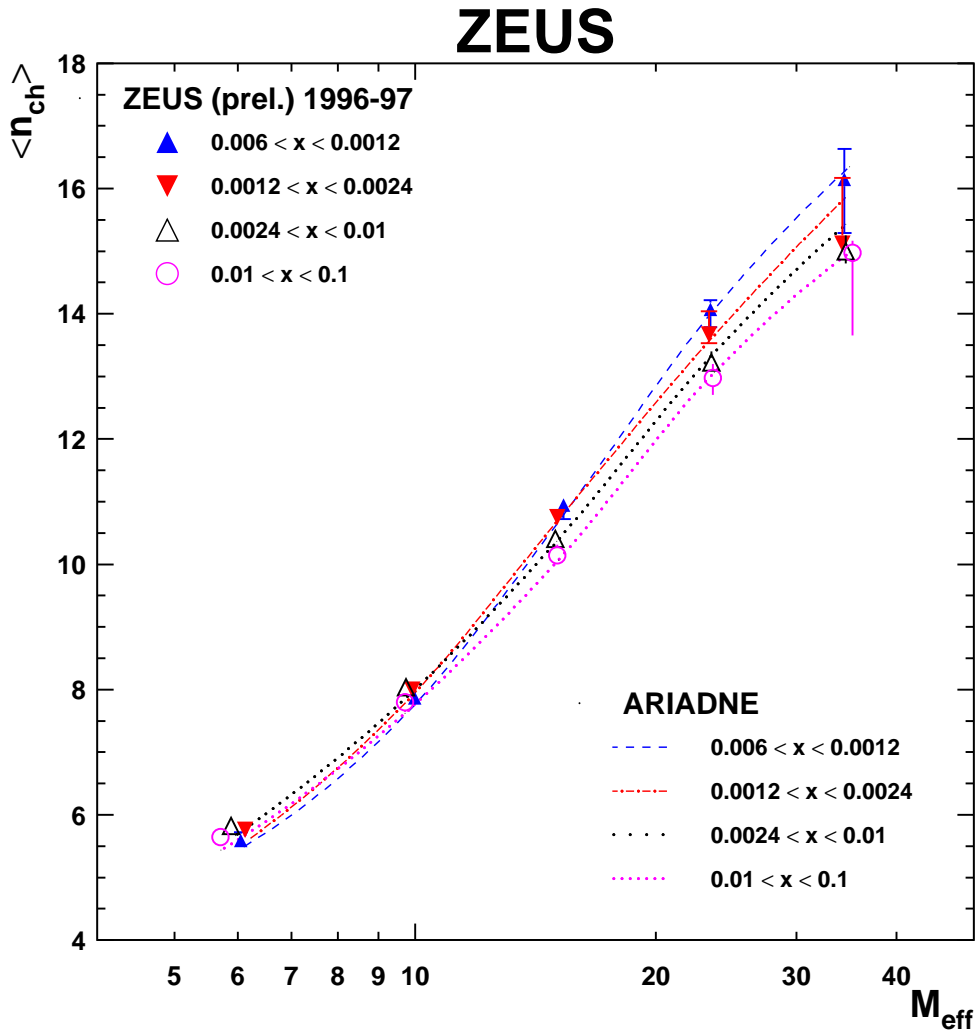


Figure 4: $\langle n_{ch} \rangle$ vs M_{eff} for different x regions together with predictions from ARIADNE.

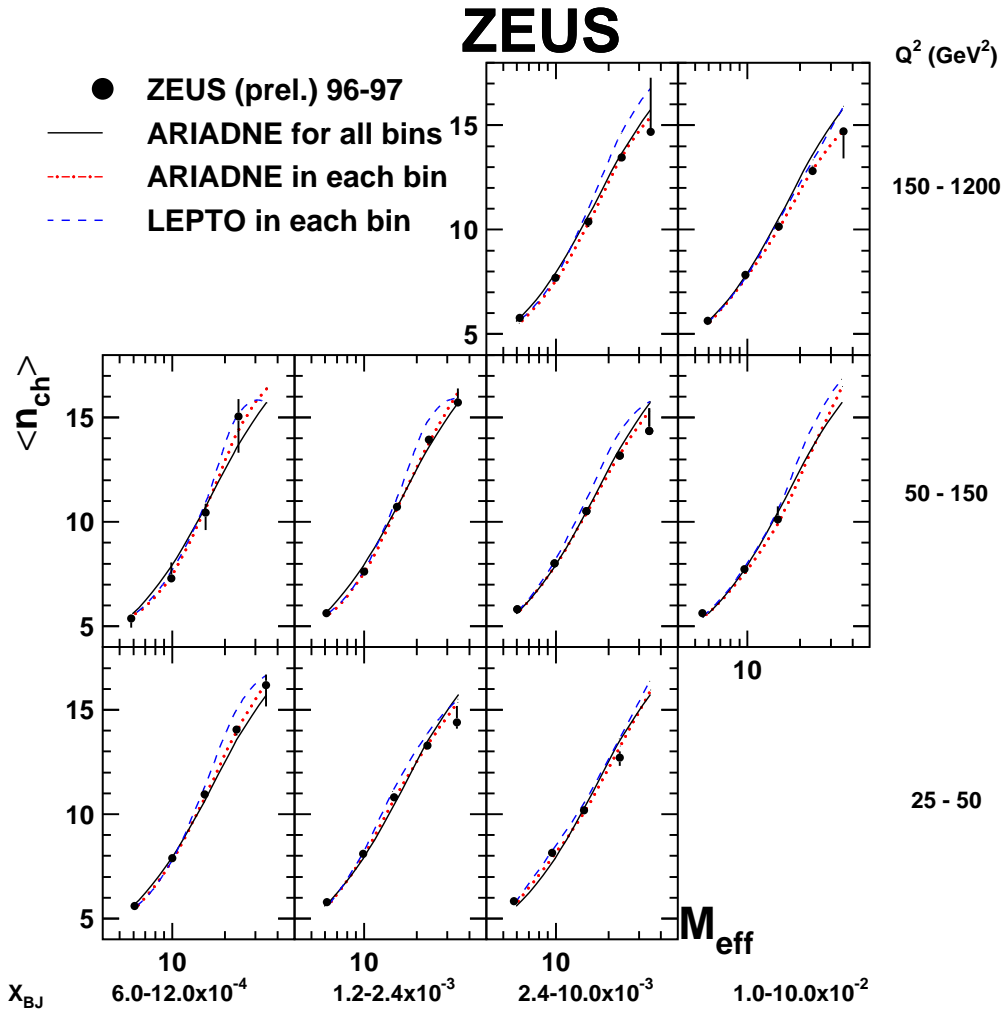


Figure 5: Figure 5 shows $\langle n_{ch} \rangle$ as a function of M_{eff} in the laboratory frame for different Q^2 and x regions together with ARIADNE and LEPTO predictions for those (x, Q^2) regions. Also the prediction of ARIADNE for the total phase space (solid line) is shown in each (x, Q^2) region.